Original Article
A dual-labeled cRGD-based PET/optical tracer for pre-operative staging and intraoperative treatment of colorectal cancer

Babs G Sibinga Mulder[1*], Henricus JM Handgraaf[1*], Danielle J Vugts[3], Claudia Sewing[3], Albert D Windhorst[3], Marieke Stammes[2], Lioe-Fee de Geus-Oei[4,5], Mark W Bordo[6], J Sven D Mieog[1], Cornelis JH van de Velde[1], John V Frangioni[6], Alexander L Vahrmeijer[1]

Departments of [1]Surgery, [2]Radiology, Leiden University Medical Center, Leiden, The Netherlands; [3]Department of Nuclear Medicine, VU Medical Center, Amsterdam, The Netherlands; [4]Department of Nuclear Medicine, Leiden University Medical Center, Leiden, The Netherlands; [5]Biomedical Photonic Imaging Group, University of Twente, Enschede, The Netherlands; [6]Curadel, LLC, Marlborough, MA, U.S.A. *Equal contributors.

Abstract: cRGD peptides target integrins associated with angiogenesis (e.g., $\alpha_v\beta_3$) and cancer, and have been used as binding ligands for both positron emission tomography (PET) and near-infrared fluorescence (NIRF) optical imaging. This study introduces the hybrid tracer cRGD-ZW800-1-Forte-[^{89}Zr]Zr-DFO, which is based on a novel zwitterionic fluorophore structure that reduces non-specific background uptake during molecular imaging of tumors. An *in vitro* binding assay was used to validate tracer performance. 10 nmol ZW800F-cRGD-Zr-DFO was injected in mice (n=7) bearing orthotopic human colorectal tumors (HT29-luc2) for tumor detection with NIRF imaging. Subsequently, ZW800F-cRGD-Zr-DFO was loaded with ^{89}Zr and 10 nmol cRGD-ZW800-1-Forte-[^{89}Zr]Zr-DFO (3 MBq) was injected in mice (n=8) for PET/CT imaging. Imaging and biodistribution was performed at 4 and 24 h. NIRF imaging was performed up to 168 h after administration. Sufficient fluorescent signals were measured in the tumors of mice injected with ZW800F-cRGD-Zr-DFO (emission peak ~800 nm) compared to the background. The signal remained stable for up to 7 days. The fluorescence signal of cRGD-ZW800-1-Forte-[^{89}Zr]Zr-DFO remained intact after labeling with ^{89}Zr. PET/CT permitted clear visualization of the colorectal tumors at 4 and 24 h. Biodistribution at 4 h showed the highest uptake of the tracer in kidneys and sufficient uptake in the tumor, remaining stable for up to 24 h. A single molecular imaging agent, ZW800F-cRGD-[^{89}Zr]Zr-DFO, permits serial PET and NIRF imaging of colorectal tumors, with the latter permitting image-guided treatment intraoperatively. Due to its unique zwitterionic structure, the tracer is rapidly renally cleared and fluorescent background signals are low.

Keywords: Hybrid tracer, colorectal cancer, molecular imaging, PET imaging, near-infrared fluorescence imaging, cRGD

Introduction

Up to 50% of patients diagnosed with colorectal cancer have either obvious or occult metastases. Initially the liver tends to harbor metastases, but peritoneal and pulmonary metastases arise as well, either synchronously or metachronously [1]. Patients with metastases require a different form of therapy (e.g. liver metastasectomy, HIPEC, palliative treatment) compared to those without. Therefore, selection of truly non-metastatic patients who will benefit from curative-intended surgery is of paramount importance. For those receiving su-

rgery, complete resection of the primary tumor with minimal morbidity is the goal. Although resection of primary tumors in the upper colon is straightforward, lower rectal resections are extremely difficult when preservation of rectal function is intended [2].

Currently, distinguishing fibrosis, inflammation, and viable tumor tissue remains difficult both preoperatively and intraoperatively, especially in patients who received neoadjuvant chemoradiotherapy. As a consequence, even patients with a pathological complete response need to undergo resection, with potentially major com-
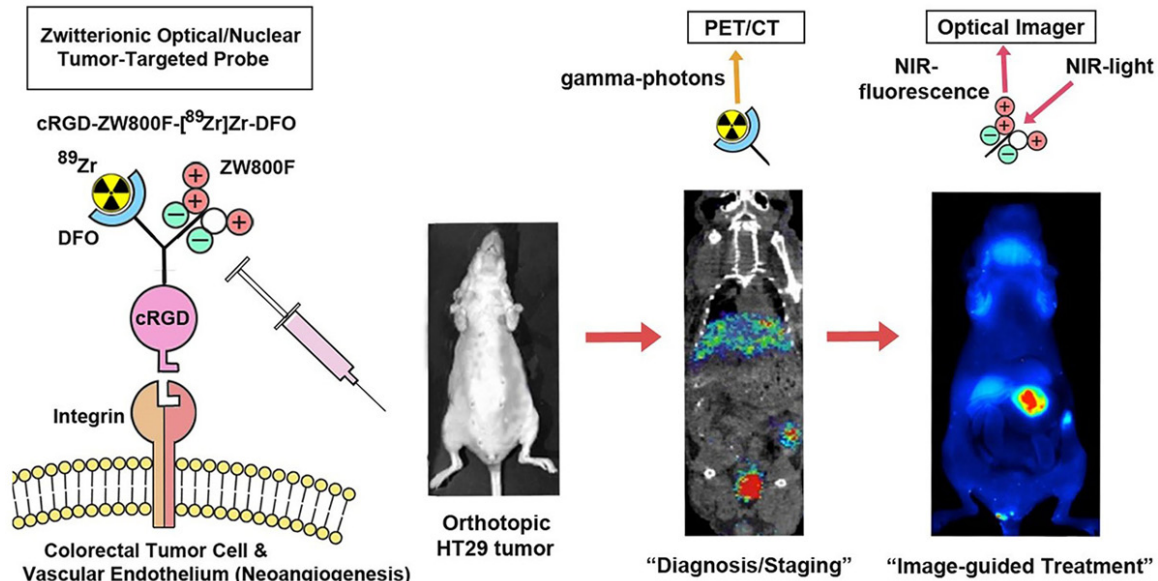
Figure 1. Study design and purposes.

plications, or an ostomy, as a result. During surgery, differentiation between malignant and benign tissue is mostly performed by visual inspection and palpation, being subjective and inaccurate. Near-infrared fluorescence (NIRF) imaging is an optical technique that permits real-time visualization of tumors during surgery using targeted fluorescent tracers [3]. Several clinical studies have demonstrated successful intraoperative identification of various tumor types [4-6]. However, NIRF imaging has an important drawback; it has a limited depth penetration of approximately 5-8 mm [7, 8]. Therefore, small metastatic tumor deposits located deeper or outside the surgeon's field of view cannot be directly identified.

To improve the management of patients diagnosed with colorectal cancer, biomedical imaging needs to meet two main requirements: 1) accurate identification of metastatic disease to preoperatively select those patients who will ultimately benefit from surgery, and, 2) real-time visualization of tumor margins in order to minimize surgical morbidity. Furthermore, obtaining market approval for even a single drug typically costs hundreds of millions of dollars and over seven years of time. There is therefore great need to develop single contrast agents (drugs) that have more than one indication [9].

Several prior reports have combined radioscintigraphy and optical imaging to perform these tasks. The first *ex vivo* study with dual-labeled

girentuximab, an antibody targeting carbonic anhydrase IX (CAIX), demonstrated that the combination of radionuclide (SPECT) and fluorescence imaging is feasible [10]. Full-length antibodies have long serum half-lives, though, resulting in non-specific background fluorescence after injection, and imaging possible only 4-7 days later. In addition, they have the potential for adverse immunological reactions, and are costly to produce.

This paper focuses on a small molecule imaging agent that can be used to improve the care of colorectal cancer patients. This agent is based on the tripeptide Arg-Gly-Asp (RGD), which targets various integrins ($\alpha_v\beta_1$, $\alpha_v\beta_3$, $\alpha_v\beta_5$, $\alpha_v\beta_6$, $\alpha_v\beta_8$, $\alpha_5\beta_1$, $\alpha_8\beta_1$ and $\alpha_{IIb}\beta_3$), some of which are overexpressed on tumor cells and tumor-associated vascular endothelium, correlating with neoangiogenesis [11]. Indeed, multiple tumor types have successfully been identified in several phase I and II clinical trials with RGD-based PET tracers [12-14]. In our previous pre-clinical study [15], cyclic RGD (cRGD) was conjugated to the near-infrared (NIR) fluorophore ZW800-1. Intravenous administration of cRGD-ZW800-1 permitted *in vivo* fluorescence imaging of multiple tumor types in mice. A clinical study investigating cRGD-ZW800-1 in patients is currently ongoing (NL6250805817).

ZW800-1 Forte is a novel zwitterionic NIR fluorophore that has the potential to further improve the tumor-to-background ratio because
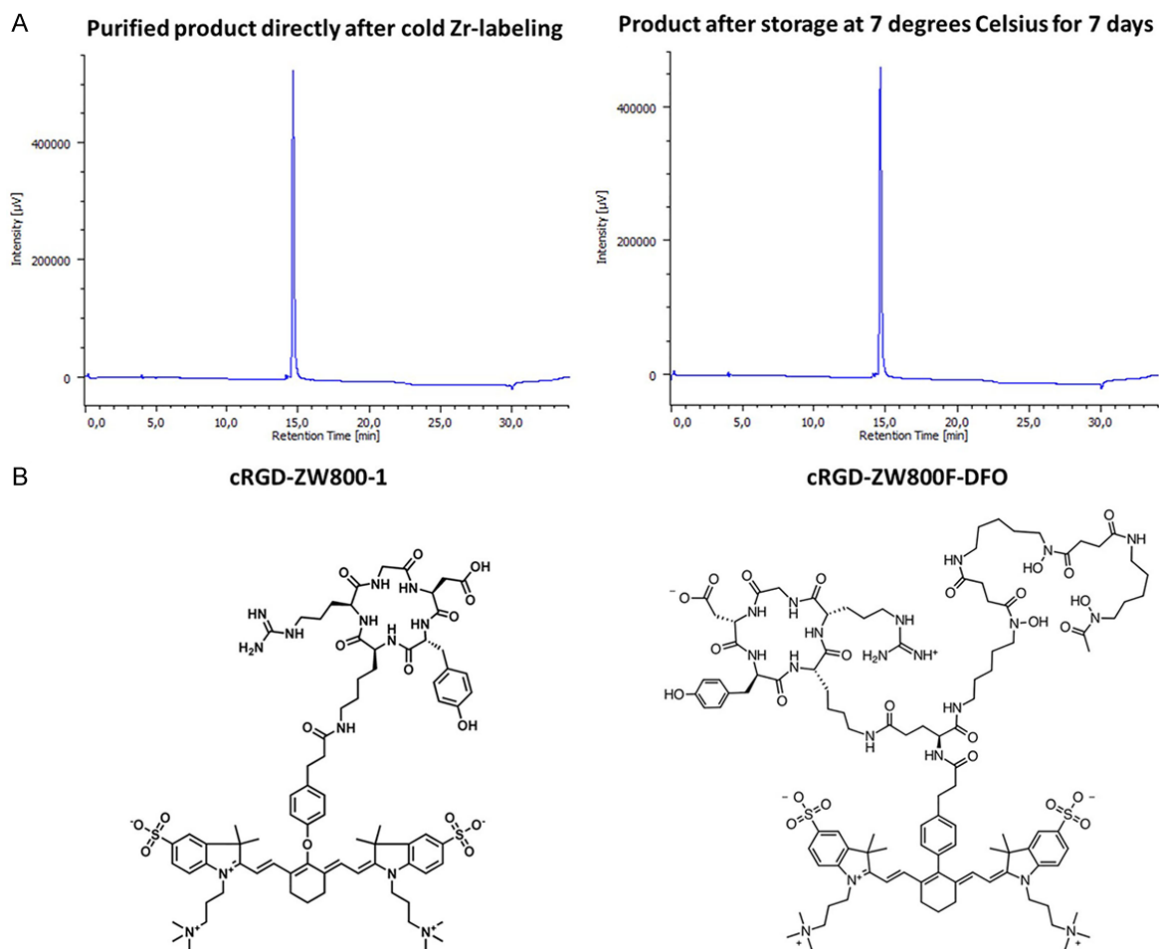
Figure 2. Stability results and chemical structure. A: Stability results over 7 days. B: Chemical structures.

of its unusually high stability *in vivo* [16]. A disadvantage of the previously described cRGD-ZW800-1 agent for use with long half-life tracers, such as [89]Zr, is its short-lived stability in serum. We therefore focus in this paper on a hybrid tracer with a more stable NIR fluorophore variant ZW800-1 Forte (ZW800F), which retains the zwitterionic motif known to reduce non-specific background in non-tumor tissues [17]. We aim to assess the feasibility to perform PET and NIR fluorescence imaging of tumors with a single injection of ZW800F-cRGD-Zr-DFO.

Methods

Figure 1 gives an overview of the study design and study purposes.

Tracer synthesis and labeling procedures

Synthesis of tracer cRGD-ZW800-1-Forte-[89Zr]Zr-DFO (cRGD-ZW800F-[89Zr]Zr-DFO), and labeling procedures are extensively described in the Supplementary Data. In short, commercially available deferoxamine (DFO) was pre-loaded and coupled to an activated boc-L-glutamic acid 1 tert-butyl ester (NHS-ester) to produce Boc-Glu(OtBu)-DFO[Fe]. The near-infrared contrast agent ZW800F was conjugated to the L-GLU-DFO[Fe] compound using a pre-activated NHS-ester. The remaining carboxyl group on the glutamic acid was converted into a TFP-ester using EDC/TFP in a MES buffer. The TFP-ester was reacted with commercially available cRGDyK to produce ZW800F-Glu(cRGDyK)-DFO[Fe]. Hereafter, 0.49 mL 0.5 M HEPES and 20 µL 2 mM cRGD-DFO-ZW800F were added to 100 µL 1 M oxalic acid containing 56.3 MBq of zirconium (mixed and reacted with 37 µL 0.9% NaCl and 45 µL 2M Na_2CO_3) and applied to a tC18 Sep-Pak, which was preconditioned with 10 mL ethanol and 10 mL water. After washing and collection of the product it was formulated to achieve a dose of 10 nmol/3 MBq ZW800F-

cRGD-[^{89}Zr]Zr-DFO per mouse, and was immediately injected. For preparation of ZW800F-cRGD-Zr-DFO 100 µL 1 M oxalic acid containing 400 nmol (2 equivalents) of zirconium was used (mixed and reacted with 345 µL 0.9% NaCl and 45 µL 2 M Na$_2$CO$_3$). Stability results are presented in **Figure 2A**.

The absorbance peak of the previously described cRGD-ZW800-1 is 773 nm [15]. The hybrid tracer ZW800-1 Forte variant has two absorbance peaks, a dominant one at 754 nm and a minor one at 680 nm. DFO was used to enable radiolabeling with the isotope zirconium-89. Because of its long half-life, ^{89}Zr has the major advantage of permitting imaging long after injection, when most background has cleared from the body. To match the long radioisotope half-life, the ZW800-1 Forte variant was used instead of ZW800-1. Chemical structures are displayed in **Figure 2B**.

In vitro binding assay

To evaluate the binding capacity of ZW800F-cRGD-Zr-DFO *in vitro*, the human colorectal cell line HT29-luc2 was used. Experiments were performed in triplicate. The cells were plated in a 96-well plate at a density of ~40,000 cells per well. At 90-100% confluence, cells were washed and incubated with various concentrations of ZW800F-cRGD-DFO at 37°C for 1 h. The cells were then washed. Subsequently, the cells were imaged using the Odyssey NIR scanner (LI-COR Biosciences, Lincoln, Nebraska; 800 nm channel) to quantify the fluorescence intensity. Next, cells were permeabilized with a 40/60 mixture of acetone and methanol followed by a washing step and 5 minutes incubation with ToPro3 (1/2000, Invitrogen), a far-red fluorescent dye. The wells were then washed again and imaged with the Odyssey scanner (700 nm channel) to quantify the number of cells in each well. No negative cell line could be used, because none of the cells are negative for cRGD-binding integrins. For example, the $α_vβ_3$ negative cell line HT-29 shows high expression of integrin $α_vβ_5$ [15].

In vivo tumor model

For *in vivo* PET and fluorescence imaging, the previously described orthotopic colorectal tumor model with HT29-luc2 cells was used [15, 18]. In short: six week-old athymic female mice

(CD1-Foxn1nu, Charles River Laboratories, Wilmington, MA, U.S.A.) were housed in ventilated cages. To induce subcutaneous tumors, colorectal cancer cells (HT-29) were injected at 4 sites on the back (500,000 cells per spot). Subsequently, these colorectal tumor cells were transplanted to the colons of fresh mice, as described by Tseng *et al.* [19]. Tumor growth and potential metastases were checked regularly using luciferin and *in vivo* bioluminescence imaging with the IVIS Spectrum (In Vivo Imaging System, PerkinElmer, Waltham, MA, U.S.A.). The Animal Welfare Committee of Leiden University Medical Center approved all animal experiments for animal health, ethics, and research. All animals received humane care and maintenance in compliance with the "Code of Practice Use of Laboratory Animals in Cancer Research" (Inspectie WandV, July 1999).

Fluorescence imaging

Evaluation of fluorescence imaging with ZW-800F-cRGD-Zr-DFO was performed with zirconium-90, a non-radioactive isotope, this was done to meet the radiation hygiene requirements for the optical imaging facility. Animals were imaged using the Pearl® imager (LICOR, Lincoln, NE, U.S.A.). The Pearl® imager uses an excitation laser of 785 nm and detects all fluorescence above 800 nm. Based on previously achieved results with cRGD-ZW800-1, all mice were imaged at 4 h and 24 h post injection [15]. Tumor-to-background ratios (TBRs) were calculated by dividing the tumor signal by the background signal (colon without tumor). After sacrificing the mice, all organs were collected and imaged using the Pearl® to evaluate the biodistribution based on fluorescence signals.

In vivo comparison of cRGD-ZW800-1 and ZW800F-cRGD-Zr-DFO

For evaluation of the stability and tumor-specificity of ZW800F-cRGD-Zr-DFO, the TBRs and fluorescence signal in the tumor obtained with the hybrid tracer were compared with the previously reported results with ZW800-cRGD-1 [15]. In that study, mice bearing orthotopic HT29-luc2 tumors were injected with the optimal dose of 10 nmol cRGD-ZW800-1 and imaged at 4 h and 24 h post injection. Therefore, seven mice bearing orthotopic HT29-luc2 tumors were injected with 10 nmol ZW800F-
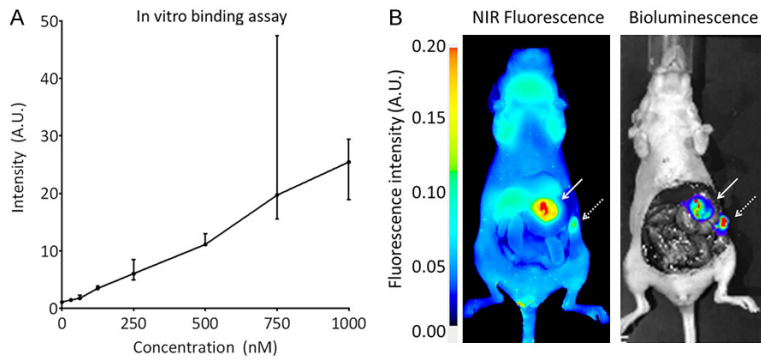
Figure 3. Binding of ZW800F-cRGD-DFO to HT-29 colorectal tumor cells. A: *In vitro* binding assay (median and range). B: *In vivo* binding of ZW800F-cRGD-Zr-DFO to the tumor (white arrow) and a peritoneal metastasis (dashed arrow) at 4 h after injection. NIRF imaging (Pearl) is in concordance with bioluminescence signals (IVIS).
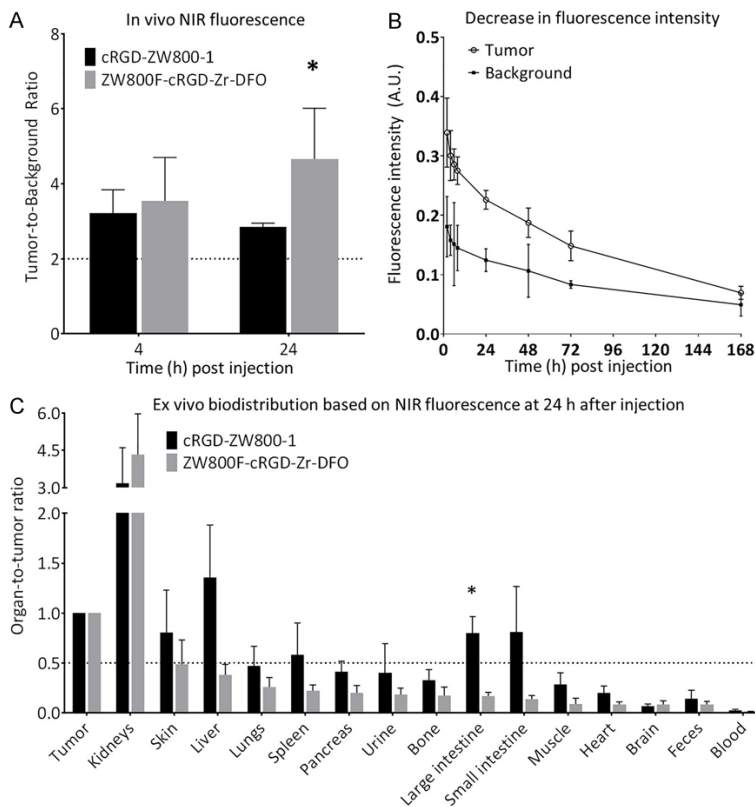

Figure 4. Comparison of cRGD-ZW800-1 and ZW800F-cRGD-DFO. A: The TBRs obtained with the ZW800F-cRGD-Zr-DFO were significantly higher at 24 h post injection (P=0.03). B: Tumor-specific signals of ZW800F-cRGD-DFO remained above 50% for up to 2 days after injection and detectable up to 7 days after injection. C: Organ-to-tumor ratios of cRGD-ZW800-1 compared to ZW800F-cRGD-Zr-DFO at 24 h after injection. The ratios are lower and more favorable for ZW800F-cRGD-Zr-DFO. *: significant differences.

rescence intensity (arbitrary units; AU) at 24 h compared to 4 h and TBRs were calculated. To assess the stability of the fluorescence signals *in vivo*, mice bearing subcutaneous HT29-luc2 tumors were injected with 10 nmol ZW800F-cRGD-Zr-DFO. The signals in the tumors and background were measured up to 168 h post injection with the Pearl® imager. Furthermore, a complete biodistribution was performed and assessed with the Pearl® imager at 24 h (n=3). The fluorescence signals of the organs compared to the tumor (organ-to-tumor ratio; OTR) of both tracers were evaluated. Because of the differences in excitation wavelengths of ZW800-1 and ZW800F and the fixed excitation wavelength of the Pearl® imager, the TBRs and the OTRs were compared instead of the fluorescence intensity of the tracers.

PET/CT

Animals were imaged with a dedicated small animal NanoPET/CT scanner (Mediso Ltd., Hungary) at VU University Medical Center. Eight mice bearing orthotopic HT29-luc2 tumors were each injected with 10 nmol cRGD-ZW800F-[89Zr]Zr-DFO (3 MBq). Mice were anesthetized by inhalation of 2% isoflurane and scanned at 1, 4 and 24 h post injection. A CT scan was acquired prior to the PET scan and was used for morphological correlation and for attenuation and scatter correction purposes. Reconstruction was performed with a fully 3-dimensional (3-D) reconstruction (Tera-Tomo; Mediso Ltd., Hungary) with four iterations and six subsets, resulting in an isotropic 0.4 mm voxel dimension. The scanner was
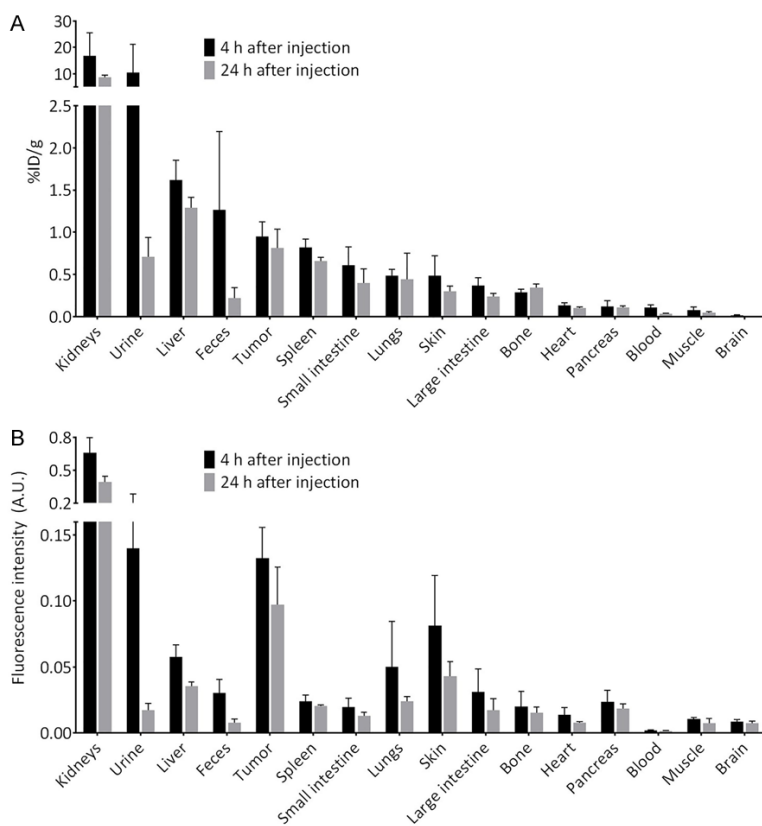
cRGD-Zr-DFO. Bioluminescence imaging was performed with luciferin and the IVIS Spectrum to compare the size of each orthotopic HT29-luc2 tumor. The percentage decrease in fluo-

Figure 5. Biodistribution studies. A: Biodistribution of cRGD-DFO[⁸⁹Zr]-ZW800F measured with the gamma counter. B: Biodistribution of ZW800F-cRGD-Zr-DFO measured with fluorescence imaging (Pearl).

son of TBRs of the Pearl®, and comparison of fluorescence intensity of tumors, was determined using an independent t-test. Differences in the biodistribution were calculated by two-way analysis of variance (ANOVA). Group means were calculated for continuous data and medians were calculated for discrete data (scores). Test statistics were calculated on the basis of exact values for means and pooled variances. All tests were two-sided and in all an alpha of 5.0% was used.

Results

Stability of cRGD-ZW800F-[⁸⁹Zr]Zr-DFO

HPLC at 780 nm of ZW800F-cRGD-Zr-DFO demonstrated a stable product up to 7 days after labeling with ⁸⁹Zr (**Figure 2A**).

In vitro binding assay

cross-calibrated with the dose calibrator and well counter, enabling the derivation of accurate standard uptake value (SUV) measures. Biodistribution was performed at 4 h (n=4) and 24 h (n=4) post-injection. After sacrificing the mice, all organs and several tissues were excised to determine the percentage of the injected dose per gram (%ID/g) with the gamma counter to evaluate biodistribution. Tumor visualization and biodistribution with NIRF imaging using ZW800F-cRGD-Zr-DFO were compared with PET/CT using cRGD-ZW800F-[⁸⁹Zr]Zr-DFO.

Statistical analysis

GraphPad Prism software (version 7.0, GraphPad Software Inc., La Jolla, California, U.S.A.) was used for statistical analyses. All values were reported using mean and standard deviation, unless otherwise described. For all *in vivo* studies at least three mice per group were included in order to be able to perform statistical power. Statistical significance for compari-

A binding assay with ZW800F-cRGD-Zr-DFO on HT29-luc2 cells showed an almost linear increase in fluorescence intensity with increasing concentrations (**Figure 3A**).

Comparison of cRGD-ZW800-1 and ZW800F-cRGD-Zr-DFO

Clear tumor demarcation was possible in the mice that were injected with ZW800F-cRGD-Zr-DFO. **Figure 3B** shows the concordance between the bioluminescent signal of the tumor measured with the IVIS and the fluorescent signal measured with the Pearl. In one mouse, bioluminescence showed a metastasis, which was also detected by NIR fluorescence imaging.

TBRs obtained in mice injected with ZW800F-cRGD-Zr-DFO were significantly higher (P=0.03) than those injected with cRGD-ZW800-1 at 24 h (**Figure 4A**). The fluorescence intensity of the tumor remained more stable using ZW800F-cRGD-Zr-DFO: only a decrease in intensity of 37% was observed between 4 and 24 h, com-
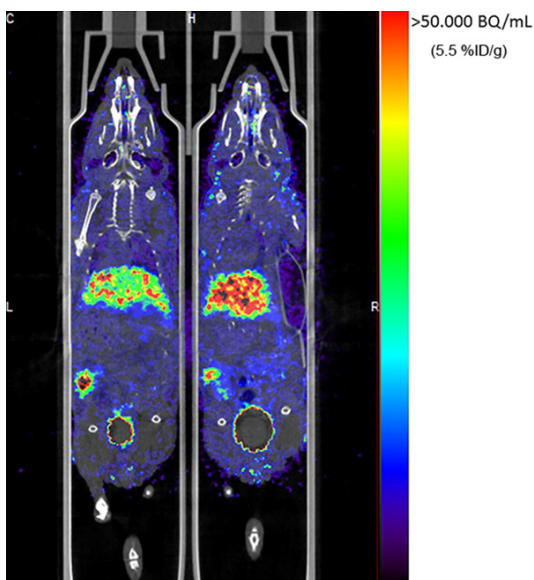
Figure 6. PET/CT of mice. Tumor specific signal of HT29 colorectal tumors (with arrow) at 4 h after injection of ZW800F-cRGD-[^{89}Zr]Zr-DFO. Also visible are the liver and bladder (dashed arrow).

pared to a 56% decrease in mice injected with cRGD-ZW800-1. In the subcutaneous HT29-luc2 tumor model, ZW800F-cRGD-Zr-DFO demonstrated a similar decrease of 33%± 5.1% at 24 h (**Figure 4B**). Approximately 50% of the fluorescence signal in tumors remained at 48 h post injection and approximately 20% of the signal remained at 7 days post injection (**Figure 3**).

The organ-to-tumor ratio (OTR) measured at 24 h (**Figure 4C**) demonstrated that conjugation of DFO did not significantly change distribution. In fact, even better results were obtained, with background in the liver, skin, intestines and all other organs at least half as fluorescent as the tumor. The only exception was the kidney, which is expected since the tracer predominantly shows renal clearance. The biodistribution of ZW800F-cRGD-Zr-DFO at 4 and 24 h, expressed in fluorescent intensity (AU) is shown in **Figure 5A, 5B**. As expected, the fluorescence signal in urine and blood decreased rapidly, as well as the signal in the kidneys.

PET imaging and biodistribution of cRGD-ZW800F-[^{89}Zr]Zr-DFO

PET/CT imaging at 4 h permitted visualization of colorectal tumors of mice injected with cRGD-ZW800F-[^{89}Zr]Zr-DFO (**Figure 6**). Based

on the gamma counter, biodistribution at 4 h after injection showed the highest uptake of the tracer in kidneys (16.8±8.6% ID/g) followed by urine, liver, colon content and tumor (0.9±0.1% ID/g). Biodistribution at 24 h showed the highest uptake of the tracer in kidneys (8.6±1.0% ID/g) followed by liver and tumor (0.8±0.2% ID/g). **Figure 3** demonstrates the biodistribution of cRGD-ZW800F-[^{89}Zr]Zr-DFO in all organs at 4 and 24 h post injection; the %ID/g strongly decreased in urine (-93%), colon content (-82%), blood (-70%), and kidneys (-48%), while it only mildly decreased in liver (-20%) and tumor (-14%).

Discussion

This study demonstrates the feasibility of identifying tumors pre-operatively and intraoperatively using a single ^{89}Zr-labeled or unlabeled molecule. Our hybrid tracer, cRGD-ZW800F-[^{89}Zr]Zr-DFO, permits both nuclear as well as NIRF imaging, with optimal results for each obtained at 24 h post-injection. Due to the use of the more stable variant of the zwitterionic fluorophore ZW800-1 Forte, superior results were obtained in comparison to cRGD-ZW800-1, thus enabling NIRF imaging for a longer time interval, up to seven days, and with lower background.

PET imaging using RGD-based tracers has proven to be successful in several clinical studies including multiple solid tumor types, such as breast, colorectal, pancreatic, and head and neck cancer [12, 20, 21]. For example, in a multicenter study, fluorine-18 labeled fluciclatide showed reproducibility in patients with several tumor types (e.g. renal cell carcinoma, breast cancer, rectal cancer) and no side effects were reported. Consistent with its zwitterionic chemical structure, the biodistribution of cRGD-Zr^{89}Z was satisfying due to the relatively low background activity, especially when compared to previously reported RGD results. For example, Zhai *et al.*, performed experiments with an RGD tracer, also radiolabeled with ^{89}Zr, conjugated to fusarine C (FSC) [22]. FSC is comparable to DFO but [^{89}Zr]FSC was found to be even more stable than [^{89}Zr]DFO in blood due to its cyclic structure. Nonetheless, in comparison with our tracer, their biodistribution obtained with [^{89}Zr] FSC-RGD at 4 h was less favorable: for all organs, except kidneys, a significant higher

uptake (%ID/g) was present. For spleen, intestines, heart, lung, muscle and bone, the tracer uptake of [89Zr]FSC-RGD was at least 3 times higher than the uptake of cRGD-ZW800F-[89Zr]Zr-DFO, for liver and pancreas the tracer uptake was at least twice as high for [89Zr]FSC-RGD compared to cRGD-Zr89Z. Despite the use of a more stable radiometal chelator, FSC, our biodistribution was, therefore, more favorable, even with an extra structure conjugated, the fluorophore ZW800F. Another study of Li et al., evaluating a dual-labeled RGD agent, 111In-DTPA-Lys(IRDye800)-c(KRGDf), allowing single photon emission computed tomography (SPECT) and fluorescence imaging of human melanoma xenografts [23]. The tracer distribution at both 4 and 24 h after injection was also less favorable than presented in the current study: higher uptake (%ID/g) was present in all organs, including the kidneys.

With regards to 89Zr, in the feasibility study of Heuveling et al., 89Zr-nanocolloidal albumin was locally injected in the oral cavity or neck of patients, 24 hours prior to surgery for the detection of the sentinel lymph node in oral cavity cancer [24]. Peroperatively, surgeons used a gamma probe to detect the radioactive lymph node(s).

Our vision for the use of 89Zr-labeled PET/optical tracers, such as ZW800F-cRGD-Zr-DFO, though, is to avoid radiation exposure to surgical caregivers, while also optimizing imaging results. A single injection of cRGD-ZW800F-[89Zr]Zr-DFO for both PET and optical imaging is inappropriate because the dose required for optical imaging is over 1,000-times higher than the dose required for PET imaging, which would result in an abnormally low specific activity (i.e., blocking) during PET. We avoid this problem by injecting the agent serially. All patients would receive tracer levels, typically < 1 μg of the labeled cRGD-ZW800F-[89Zr]Zr-DFO and PET would be used to select those eligible for surgery. Then, pre-operatively, unlabeled ZW800F-cRGD-Zr-DFO would be injected and NIRF imaging can be used for real-time intraoperative margin detection for treatment.

Contrast agents such as DFO-cRGD-ZW800-1 minimize the overall cost and time of market approval. Using two different molecules for pre-surgical staging and intraoperative imaging would mean double the cost and time, because each chemical entity would require separate market approval. Developing a single drug with two different indications greatly decreases both the costs and time required to have both indications available to patients. The savings could be as high as $ 100 M and 7 years [9].

Finally, another advantage of our dual-labeled zwitterionic tracer is its renal clearance, which bypasses biliary excretion and renders the abdominal cavity non-fluorescent. This should improve identification of primary tumor margins from a variety of tumor, such as colorectal, liver, and pancreas, as well as identification of occult intra-abdominal metastases. Of note, despite rather rapid renal clearance of the agent, we recommend imaging at long time points, such as at 24 h post injection, in order to reduce background signal in non-target organs, and thus increase TBR, as much as possible.

Conclusion

A single molecular imaging agent, ZW800F-cRGD-[89Zr]Zr-DFO, permits serial PET and NIRF-guided treatment of colorectal tumors. The tracer is rapidly cleared via the kidneys and, due to the use of zwitterionic stable ZW800-1 Forte, fluorescent background signals are low. 89Zr-labelled tracer may be used to select patients for surgery. Subsequently, the same non-radiolabeled tracer can be used peroperatively for real-time tumor detection.

Acknowledgements

Disclosure of conflict of interest

John V. Frangioni is currently CEO of Curadel, Curadel ResVet Imaging, and Curadel Surgical Innovations, which are for-profit companies that have licensed FLARE® technology from Beth Israel Deaconess Medical Center. All other authors have no conflicts of interests or financial ties to disclose.

Address correspondence to: Alexander L Vahrmeijer, Department of Surgery, Leiden University Medic-

al Center, P.O. Box 9600, 2300 RC Leiden, The Netherlands. Tel: +31 71 5265039; E-mail: a.l. vahrmeijer@lumc.nl

References

[1] Jones RP, Kokudo N, Folprecht G, Mise Y, Unno M, Malik HZ, Fenwick SW and Poston GJ. Colorectal liver metastases: a critical review of state of the art. Liver Cancer 2016; 6: 66-71.

[2] Marr R, Birbeck K, Garvican J, Macklin CP, Tiffin NJ, Parsons WJ, Dixon MF, Mapstone NP, Sebag-Montefiore D, Scott N, Johnston D, Sagar P, Finan P and Quirke P. The modern abdominoperineal excision: the next challenge after total mesorectal excision. Ann Surg 2005; 242: 74-82.

[3] Vahrmeijer AL, Hutteman M, van der Vorst JR, van de Velde CJ and Frangioni JV. Image-guided cancer surgery using near-infrared fluorescence. Nat Rev Clin Oncol 2013; 10: 507-518.

[4] Hoogstins CE, Tummers QR, Gaarenstroom KN, de Kroon CD, Trimbos JB, Bosse T, Smit VT, Vuyk J, van de Velde CJ, Cohen AF, Low PS, Burggraaf J and Vahrmeijer AL. A novel tumor-specific agent for intraoperative near-infrared fluorescence imaging: a translational study in healthy volunteers and patients with ovarian cancer. Clin Cancer Res 2016; 22: 2929-2938.

[5] Lamberts LE, Koch M, de Jong JS, Adams ALL, Glatz J, Kranendonk MEG, Terwisscha van Scheltinga AGT, Jansen L, de Vries J, Lub-de Hooge MN, Schröder CP, Jorritsma-Smit A, Linssen MD, de Boer E, van der Vegt B, Nagengast WB, Elias SG, Oliveira S, Witkamp AJ, Mali WPTM, Van der Wall E, van Diest PJ, de Vries EGE, Ntziachristos V and van Dam GM. Tumor-specific uptake of fluorescent bevacizumab-IRDye800CW microdosing in patients with primary breast cancer: a phase i feasibility study. Clin Cancer Res 2017; 23: 2730-2741.

[6] Rosenthal EL, Warram JM, de Boer E, Chung TK, Korb ML, Brandwein-Gensler M, Strong TV, Schmalbach CE, Morlandt AB, Agarwal G, Hartman YE, Carroll WR, Richman JS, Clemons LK, Nabell LM and Zinn KR. Safety and tumor specificity of cetuximab-IRDye800 for surgical navigation in head and neck cancer. Clin Cancer Res 2015; 21: 3658-3666.

[7] Frangioni JV. New technologies for human cancer imaging. J Clin Oncol 2008; 26: 4012-4021.

[8] Teraphongphom N, Kong CS, Warram JM and Rosenthal EL. Specimen mapping in head and neck cancer using fluorescence imaging. Laryngoscope Investig Otolaryngol 2017; 2: 447-452.

[9] Nunn AD. The cost of developing imaging agents for routine clinical use. Invest Radiol 2006; 41: 206-212.

[10] Hekman MC, Boerman OC, de Weijert M, Bos DL, Oosterwijk E, Langenhuijsen JF, Mulders PF and Rijpkema M. Targeted dual-modality imaging in renal cell carcinoma: an ex vivo kidney perfusion study. Clin Cancer Res 2016; 22: 4634-4642.

[11] Desgrosellier JS and Cheresh DA. Integrins in cancer: biological implications and therapeutic opportunities. Nat Rev Cancer 2010; 10: 9-22.

[12] Beer AJ, Lorenzen S, Metz S, Herrmann K, Watzlowik P, Wester HJ, Peschel C, Lordick F and Schwaiger M. Comparison of integrin $\alpha_v\beta_3$ expression and glucose metabolism in primary and metastatic lesions in cancer patients: a PET study using ^{18}F-galacto-RGD and ^{18}F-FDG. J Nucl Med 2008; 49: 22-29.

[13] Sharma R, Kallur KG, Ryu JS, Parameswaran RV, Lindman H, Avril N, Gleeson FV, Lee JD, Lee KH, O'Doherty MJ, Groves AM, Miller MP, Somer EJ, Coombes CR and Aboagye EO. Multicenter reproducibility of ^{18}F-Fluciclatide PET imaging in subjects with solid tumors. J Nucl Med 2015; 56: 1855-1861.

[14] Kang F, Wang Z, Li G, Wang S, Liu D, Zhang M, Zhao M, Yang W and Wang J. Inter-heterogeneity and intra-heterogeneity of alphavbeta3 in non-small cell lung cancer and small cell lung cancer patients as revealed by ^{68}Ga-RGD2 PET imaging. Eur J Nucl Med Mol Imaging 2017; 44: 1520-1528.

[15] Handgraaf HJM, Boonstra MC, Prevoo HAJM, Kuil J, Bordo MW, Boogerd LSF, Sibinga Mulder BG, Sier CFM, Vinkenburg-van Slooten ML, Valentijn ARPM, Burggraaf J, van de Velde CJH, Frangioni JV, Vahrmeijer AL. Real-time near-infrared fluorescence imaging using cRGD-ZW800-1 for intraoperative visualization of multiple cancer types. Oncotarget 2017; 8: 21054-21066.

[16] Hyun H, Owens EA, Narayana L, Wada H, Gravier J, Bao K, Frangioni JV, Choi HS and Henary M. Central C-C bonding increases optical and chemical stability of NIR fluorophores. RSC Adv 2014; 4: 58762-58768.

[17] Choi HS, Gibbs SL, Lee JH, Kim SH, Ashitate Y, Liu F, Hyun H, Park G, Xie Y, Bae S, Henary M and Frangioni JV. Targeted zwitterionic near-infrared fluorophores for improved optical imaging. Nat Biotechnol 2013; 31: 148-153.

[18] Boonstra MC, Tolner B, Schaafsma BE, Boogerd LS, Prevoo HA, Bhavsar G, Kuppen PJ, Sier CF, Bonsing BA, Frangioni JV, van de Velde CJ, Chester KA and Vahrmeijer AL. Preclinical evaluation of a novel CEA-targeting near-infrared fluorescent tracer delineating colorectal and

pancreatic tumors. Int J Cancer 2015; 137: 1910-1920.

[19] Tseng W, Leong X and Engleman E. Orthotopic mouse model of colorectal cancer. J Vis Exp 2007; 484.

[20] Beer AJ, Kessler H, Wester HJ and Schwaiger M. PET Imaging of Integrin alphaVbeta3 Expression. Theranostics 2011; 1: 48-57.

[21] Beer AJ, Schwarzenbock SM, Zantl N, Souvatzoglou M, Maurer T, Watzlowik P, Kessler H, Wester HJ, Schwaiger M and Krause BJ. Non-invasive assessment of inter-and intrapatient variability of integrin expression in metastasized prostate cancer by PET. Oncotarget 2016; 7: 28151-28159.

[22] Zhai C, Summer D, Rangger C, Franssen GM, Laverman P, Haas H, Petrik M, Haubner R and Decristoforo C. Novel bifunctional cyclic chelator for ^{89}Zr labeling-radiolabeling and targeting properties of RGD conjugates. Mol Pharm 2015; 12: 2142-2150.

[23] Li C, Wang W, Wu Q, Ke S, Houston J, Sevick-Muraca E, Dong L, Chow D, Charnsangavej C and Gelovani JG. Dual optical and nuclear imaging in human melanoma xenografts using a single targeted imaging probe. Nucl Med Biol 2006; 33: 349-358.

[24] Heuveling DA, Karagozoglu KH, Van Lingen A, Hoekstra OS, Van Dongen G and De Bree R. Feasibility of intraoperative detection of sentinel lymph nodes with 89-zirconium-labelled nanocolloidal albumin PET-CT and a handheld high-energy gamma probe. EJNMMI Res 2018; 8: 15.

Supplementary Data

Tracer synthesis

Commercially available deferoxamine (DFO) was pre-loaded using iron(III) chloride. In a single pot reaction, boc-L-glutamic acid 1 tert-butyl ester was activated using dipyrrolidino(N-succinimidyloxy)carbenium hexafluorophosphate (HSPyU) and DIEA to produce an NHS-ester. The pre-loaded DFO was then added to the reaction pot to produce Boc-Glu(OtBu)-DFO[Fe]. The use of iron prevents HSPyU from reacting with the three hydroxamate groups of DFO. Protecting groups on the amino acid were removed using a combination of TFA and DCM at room temperature. The target molecule was purified using solid phase extraction. A small molar equivalency of $FeCl_3$ was used during a wash step to ensure that the DFO is complexed to iron(III). The near-infrared contrast agent ZW800F was conjugated to the L-GLU-DFO[Fe] compound using a pre-activated NHS-ester. The target compound ZW800F-Glu(COOH)-DFO[Fe] was purified using solid phase extraction and concentrated under vacuum. The remaining carboxyl group on the glutamic acid was converted into a TFP-ester using EDC/TFP in a MES buffer. The TFP-ester product was purified using solid phase extraction and concentrated under vacuum. The TFP ester was used due to its increased stability to moisture during the drying process. The TFP-ester was reacted with commercially available cRGDyK to produce ZW800F-Glu(cRGDyK)-DFO[Fe]. The peptide bond is formed in DMSO under a basic environment. During purification using solid phase extraction, EDTA is used to remove the iron from the DFO. The synthesis of cRGD-ZW800-1 was previously described [1].

Preparation of ZW800F-cRGD-[^{89}Zr]Zr-DFO

100 µL 1 M oxalic acid containing 56.3 MBq of zirconium was mixed with 37 µL 0.9% NaCl and 45 µL 2 M Na_2CO_3 and reacted for 10 minutes. Hereafter 0.49 mL 0.5 M HEPES and 20 µL 2 mM cRGD-DFO-ZW800F were added bringing the total volume to 1 mL which was reacted for 60 minutes at room temperature. The reaction mixture was applied to a tC18 Sep-Pak, which was preconditioned with 10 mL ethanol and 10 mL water. Next the Sep-Pak was washed twice with 8 mL water, followed by elution of the Sep-Pak with 60/40 ethanol/50 mM NaOAc pH 5.0. The product was collected in 0.5 mL (fraction 3 and 4 from eluted cartridge) in a radiochemical yield of 88%. Next the product was formulated to achieve a dose of per mouse of 10 nmol (dose chosen based on previous experience [2])/3 MBq ZW800F-cRGD-[^{89}Zr]Zr-DFO in 150 µL injection volume and was immediately injected. The radiochemical purity was 99.5% base on iTLC using 50 mM EDTA as eluent.

Preparation of ZW800F-cRGD-Zr-DFO

100 µL 1 M oxalic acid containing 400 nmol (2 equivalents) of zirconium was mixed with 345 µL 0.9% NaCl and 45 µL 2 M Na_2CO_3 and reacted for 10 minutes. Hereafter, 0.5 mL 0.5 M HEPES and 100 µL 2 mM cRGD-DFO-ZW800F (200 nmol) were added bringing the total volume to 1090 µL which was reacted for 60 minutes at room temperature. The reaction mixture was applied to a tC18 Sep-Pak, which was preconditioned with 10 mL ethanol and 10 mL water. Next the Sep-Pak was washed twice with 8 mL water, followed by elution of the Sep-Pak with 60/40 ethanol/50 mM NaOAc pH 5.0. The product was collected in 0.5 mL (fraction 3 and 4 from eluted cartridge) in a yield of 78% (determined by HPLC using an Alltima C-18 column). Next the product was formulated to achieve a dose of per mouse of 10 nmol ZW800F-cRGD-Zr-DFO in 120 µL injection volume. The stability of the product was assessed for 7 days by high-performance liquid chromatography (HPLC) (**Figure 2**).

References

[1]   Choi HS, Gibbs SL, Lee JH, Kim SH, Ashitate Y, Liu F, Hyun H, Park G, Xie Y, Bae S, Henary M, Frangioni JV. Targeted zwitterionic near-infrared fluorophores for improved optical imaging. Nat Biotechnol 2013; 31: 148-53.

[2]   Handgraaf HJM, Boonstra MC, Prevoo HAJM, Kuil J, Bordo MW, Boogerd LSF, Sibinga Mulder BG, Sier CFM, Vinkenburg-van Slooten ML, Valentijn ARPM, Burggraaf J, van de Velde CJH, Frangioni JV, Vahrmeijer AL. Real-time near-infrared fluorescence imaging using cRGD-ZW800-1 for intraoperative visualization of multiple cancer types. Oncotarget 2017; 8: 21054-66.